THE JOURNAL OF BIOLOGICAL CHEMISTRY VOL. 284, NO. 50, pp. 34954–34963, December 11, 2009
© 2009 by The American Society for Biochemistry and Molecular Biology, Inc. Printed in the U.S.A.

Cytoplasmic ACK1 Interaction with Multiple Receptor Tyrosine Kinases Is Mediated by Grb2

AN ANALYSIS OF ACK1 EFFECTS ON Axl SIGNALING[*][S]

Received for publication, October 6, 2009 Published, JBC Papers in Press, October 8, 2009, DOI 10.1074/jbc.M109.072660

Lin Pao-Chun, Perry M. Chan, Wing Chan, and Ed Manser[1]

From the sGSK Group, Astar-Neuroscience Research Partnership, and Institute of Molecular and Cell Biology, 61 Biopolis Drive, Singapore 138673

ACK1 (activated Cdc42-associated kinase 1), a cytoplsmic tyrosine kinase, is implicated in metastatic behavior, cell spreading and migration, and epidermal growth factor receptor (EGFR) signaling. The function of ACK1 in the regulation of receptor tyrosine kinases requires a C-terminal region that demonstrates a significant homology to the EGFR binding domain of MIG6. In this study, we have identified additional receptor tyrosine kinases, including Axl, leukocyte tyrosine kinase, and anaplastic lymphoma kinase, that can bind to the ACK1/MIG6 homology region. Unlike the interaction between MIG6 and EGFR, our data suggest that these receptor tyrosine kinases require the adaptor protein Grb2 for efficient binding, which interacts with highly conserved proline-rich regions that are conserved between ACK1 and MIG6. We have focused on Axl and compared how ACK1/Axl differs from the ACK1/EGFR axis by investigating effects of knockdown of endogenous ACK1. Although EGFR activation promotes ACK1 turnover, Axl activation by GAS6 does not; interestingly, the reciprocal down-regulation of GAS6-stimulated Axl is blocked by removing ACK1. Thus, ACK1 functions in part to control Axl receptor levels. Silencing of ACK1 also leads to diminished ruffling and migration in DU145 and COS7 cells upon GAS6-Axl signaling. The ability of ACK1 to modulate Axl and perhaps anaplastic lymphoma kinase (altered in anaplastic large cell lymphomas) might explain why ACK1 can promote metastatic and transformed behavior in a number of cancers.

The non-receptor tyrosine kinase ACK1 was identified as a specific interactor of Cdc42.GTP (1). This cytoplasmic tyrosine kinase is encoded by a single gene and is related to TNK1, which is expressed in immune cells; TNK does not contain the Cdc42 binding motif (2). A related non-kinase protein, MIG6 (also called Gene 33), is induced by multiple stimuli and would appear to be part of a feedback loop that modulates EGF[2] signaling (3). Apart from the N-terminal kinase and CRIB domain, the multidomain ACK1 also contains an SH3 domain, a clathrin binding box (LIDFG), and a ubiquitin association (UBA) domain (4–7).

It has been suggested that the ACK1 kinase domain is active regardless of activation loop phosphorylation (8). The function of the SH3 and other domains in negatively regulating kinase activity has been suggested (7). At present, there is no structural information on the larger scale organization of ACK1, but one might anticipate autoinhibition by sequences outside the kinase domain in a similar manner as Src. The proline-rich C-terminal region has been identified as a region that binds adaptors, such as Grb2 (6).

ACK1 is expressed highest in brain, spleen, thymus, and liver (7) but probably is present in most cell types. The kinase is implicated in cell spreading (9) and migration through phosphorylation of $p130^{cas}$ (10). Because ACK1 is tightly coupled to the clathrin system (4, 11), a role in endocytosis is well accepted. ACK1 contains a region of high degree of homology to the EGFR binding domain of MIG6 but not found in any other protein, suggesting that these proteins are evolutionarily related. MIG6 can bind to and inhibit the EGFR family of receptor tyrosine kinase (RTK) (12, 13). This activity of MIG6 involves association with the EGFR kinase domain through two segments that can bind and prevent EGFR activation in *trans* (14). The first segment (MIG6-(337–361)) binds to the dimerization interface, whereas the second segment (residues 362–412) binds the C-lobe of EGFR. Since ACK1 has a closely related sequence that binds EGFR, one anticipates that its mode of action is similar. ACK1 is reported to interact preferentially with activated EGFR (5).

The role of ACK1 in receptor endocytosis and vesicle dynamics is more complex (15). Overexpression of ACK1, like many multivalent clathrin-binding proteins, causes clathrin aggregation and blocks its function (4). ACK1 can affect turnover of activated EGFR and endocytosis (5, 15), but the details have yet to be resolved. In *Caenorhabditis elegans*, genetic analysis suggests that Ark-1, an orthologue of ACK, negatively regulates EGFR signaling (16). In higher organisms, ACK1 also binds PDGFR (7) and Mer kinase (17), suggesting that the kinase may be more widely involved in RTK dynamics.

Amplification of the *ACK1* gene locus is detected in a number of primary tumors, whereas overexpression of ACK1 in cancer cell lines increases their metastatic ability (18). The activity of ACK1 in enhancing the growth of the prostate cancer

* This work is supported by the GSK (Singapore) research fund.

[S] The on-line version of this article (available at http://www.jbc.org) contains supplemental Table 1 and Figs. 1 and 2.

[1] To whom correspondence should be addressed. E-mail: ed.manser@imb.a-star.edu.sg.

[2] The abbreviations used are: EGF, epidermal growth factor; EGFR, EGF receptor; SH3, Src homology 3; SH2, Src homology 2; RTK, receptor tyrosine kinase; LTK, leukocyte tyrosine kinase; siRNA, small interfering RNA; GST, glutathione *S*-transferase; PBS, phosphate-buffered saline; TRITC, tetramethylrhodamine isothiocyanate; PDGFR, platelet-derived growth factor receptor; ERK, extracellular signal-regulated kinase; MAPK, mitogen-activated protein kinase; MEK, mitogen-activated protein kinase/extracellular signal-regulated kinase kinase; HA, hemagglutinin.

line LNCaP is suggested to occur via negative regulation of Wwox (17).

In this report, we screened for the potential of new RTKs to interact with ACK1 or MIG6 via the region that these proteins share in their C termini. From this screen, we determined that a subset of RTKs only bind ACK1 well via the adaptor Grb2. Axl, leukocyte tyrosine kinase (LTK), and anaplastic lymphoma kinase (ALK) have been identified as partners for ACK1 and MIG6. Considering their position within various RTK subfamilies, LTK and ALK emerge as novel ACK1-interacting proteins. We have focused our analysis on Axl, because of the wide expression of this RTK and its importance in metastatic behavior (19). Using siRNA-mediated knockdown of ACK1 and GAS6-mediated activation of Axl, we have investigated the relationship of these two tyrosine kinases in permissive cell lines. In this respect, we highlight similarities and differences between the effects of EGFR and Axl.

EXPERIMENTAL PROCEDURES

Materials—High affinity glutathione-Sepharose beads were from GeneScript. Anti-ACK1 (A-11), anti-EGFR, anti-Myc, anti-actin, and anti-Cdc42 antibodies were from Santa Cruz Biotechnology, Inc. (Santa Cruz, CA). Anti-Axl (N-terminal) and anti-Axl (C-terminal) were from R&D Systems and Santa Cruz Biotechnology, Inc., respectively. Anti-FLAG (M2), anti-GST antibodies, and Fibronectin solution were from Sigma. Anti-Grb2, anti-phosphotyrosine (4G10), anti-Rac1 antibodies, and EGF were from Millipore/Upstate. Anti-HA antibody (12CA5) was from Roche Applied Science. Anti-phospho-Akt (Ser^{473}; 4060) and anti-phospho-ERK1/2 (Thr^{202}/Tyr^{204}; 9101) antibodies were from Cell Signaling Technology. A transwell of 8-μm pore size and 6.5-mm diameter was from Costar. Secondary antibodies used for immunofluorescence were from Molecular Probes.

Cell Culture—COS7 cells were maintained in Dulbecco's modified Eagle's medium supplemented with 10% fetal bovine serum in a 37 °C incubator with 5% CO_2. DU145 cells were cultured using RPMI supplemented with L-glutamine and 10% fetal bovine serum.

Generation of RTK Constructs—Constructs encoding the open reading frame of the kinases or complete expressed sequence tag clones were obtained from Open Biosystem. The constructs were cloned into pcDNA3 with a C-terminal FLAG tag using standard PCR protocols. The respective primers used are documented in supplemental Table 1.

Generation of ACK1, MIG6, and Grb2 Constructs—ACK T1 was constructed via PCR using the primers 5′-CTAGGATCCTGCCCGCCCTCCCTGGCGCAG-3′ and 5′-CAGGTCGACTTAAGGCACAGGCAGGGGGGT-3′, which contain flanking BamHI or SalI restriction sites. ACK T2 and T3, which were previously cloned into pXJ-FLAG vector, were recloned into pXJ-GST via BamHI/HindIII restriction sites. The MIG6 fragment was subjected to PCR using the following primers: 5′-CACGGATCCGCTGGCTCCTTTAACAAGCCA-3′ and 5′-CGCCTCGAGCTAAGGAGAAACCACATAGGA-3′. The amplified products were cloned into pXJ-GST via BamHI/XhoI restriction sites. Grb2 mutants were created via two-step PCR mutagenesis and sequenced to confirm the mutations. The mutated full-length products were cloned into pXJ-HA via BamHI/XhoI sites.

DNA Transfection and RNA Interference—COS7 cells were transfected at 80–90% confluence with Lipofectamine 2000 (Invitrogen) at a ratio of 1 μg of DNA to 3 μl of reagent and in conditions according to the manufacturer's instructions. Cells were harvested 48 h post-transfection. For RNA interference, a ratio of 20 pmol to 3 μl of the transfection reagent was used. The siRNAs were synthesized by Invitrogen. Cells were treated with control siRNA and siRNAs against ACK1, Grb2, and Cdc42. The siRNA sequences were as follows: ACK siA (5′-AAGAUGGUGACAGAGCUGGCA-3′), ACK siA_2 (5′-GAAGAUGGUGACAGAGCUGGCACTT-3′), ACK siC (5′-GCCUGUCCCACUUUGAGUAdTdT-3′), and Grb2 siRNA (5′-CAUGUUUCCCCGCAAUUAUdTdT-3′). Cells were typically transfected for 24 h before serum starvation for another 24 h before harvest.

Synthesis of Recombinant GAS6—cDNA of human GAS6 (Open Biosystem) was subjected to PCR using the primers 5′-AATGGATCCACCATGGCCCCTTCGCTCTCG-3′ and 5′-TAAGCGGCCGCAAGGCTGCGGCGGG-3′. The amplified product was cloned into C-terminal His tag pcDNA3 vector via BamHI/NotI sites. The construct was transfected into HEK293 cells via Lipofectamine 2000 (Invitrogen) for 4 h before changing into serum-free medium containing 4 μM menadione sodium bisulfite (an analog of Vitamin K). The transfected cells were allowed to express and secrete the recombinant GAS6 into the medium for 48 h. The medium with the secreted GAS6 was purified via a nickel bead (Ni^{2+}-nitrilotriacetic acid, Qiagen)-based His-tagged purification method. Briefly, the medium was reconstituted into a final concentration of 50 mM NaH_2PO_4, 500 mM NaCl, 10 mM imidazole, 0.1% Triton X-100 and adjusted to pH 8.0. The medium was allowed to flow through the nickel bead column and washed extensively with washing buffer of similar salt concentrations. Recombinant GAS6 was eluted from the beads with 300 mM imidazole and dialyzed against 1× PBS. The protein concentration was measured via Bio-Rad protein assay.

Overlays with [γ-^{32}P]GTP-labeled Proteins—The SH3 array filters were purchased from Panomics (Array II; catalog number MA3012). The fusion proteins of GST-ACK1-(732–761) and GST-ACK1-(771–800) were labeled as described previously (20) and used at 10 μg/ml.

Pull-down Assays, Ligand Stimulation, and Western Blot Analysis—For RTK interaction analysis, cells were pretreated with 500 μM of sodium orthovanadate for 30 min before cell lysis. In these pull-down assays, the cells were washed with cold PBS and harvested with Triton lysis buffer of 50 mM Hepes, pH 7.3, 1 mM EDTA, 0.1 mM dithiothreitol, 10% glycerol, 1% Triton X-100, 1.5 mM $MgCl_2$, 10 mM NaF, 150 mM NaCl, 1 mM $NaVO_3$, protease inhibitor mixture, and 20 mM glyceraldehyde β-glycerophosphate. The lysates were sonicated and spun in a microcentrifuge at 14,000 rpm for 10 min. The supernatants were incubated with GST beads for at least 2 h at 4 °C before extensive washing with the same lysis buffer and eluted with sample buffer. For EGF/GAS6 stimulation, COS7 cells were serum-starved overnight before stimulation with EGF (100 ng/ml) or GAS6 (200 or 400 ng/ml).The cells were then washed with cold

PBS and lysed with radioimmune precipitation lysis buffer (0.1 M Tris, pH 7.4, 0.15 M NaCl, 1% Triton X-100, 0.5% deoxycholate, 0.1% SDS, 5% glycerol, 1 mM phenylmethylsulfonyl fluoride, 20 mM β-glycerophosphate, and protease inhibitor mixture). The lysates were sonicated and spun in a microcentrifuge at 14,000 rpm for 10 min. Protein sample buffer was added into the supernatants and boiled before SDS-polyacrylamide gel electrophoresis. All of the protein samples were subjected to SDS-PAGE and transferred onto polyvinylidene difluoride membrane. The membranes were blocked with 3% bovine serum albumin in 0.05% Tween 20, Tris buffer for 30 min and incubated with primary antibodies diluted in 3% bovine serum albumin, 0.05% Tween 20, Tris buffer for at least 1 h at room temperature or overnight at 4 °C. The membranes were washed with 0.05% Tween 20, Tris buffer and incubated with anti-rabbit/goat/mouse horseradish peroxidase secondary antibodies for 1 h at room temperature. After washing, signals were visualized with enhanced chemiluminescence detection reagents (Super Signal from Thermo Scientific).

Activated Axl Detection and Endogenous Axl Immunoprecipitation—A phosphopeptide encompassing the Tyr^{702}/Tyr^{703} residues of the Axl activation loop was synthesized: Ac-CKIYNGDpYpYRQGR (where pY represents phosphotyrosine; Genemed Synthesis, Inc.). Phospho-Tyr^{702}/Tyr^{703}-specific antibodies were purified from immunized rabbit sera using immobilized peptide. To detect endogenous Axl-ACK1 complexes, serum-starved COS7 cells were treated with GAS6 (400 ng/ml) and lysed at various time points. Endogenous Axl was immunoprecipitated with the goat Axl antibodies/Protein G beads for 4 h at 4 °C and washed three times before elution with sample buffer. The protein samples were then subjected to SDS-PAGE and Western blot analysis.

Transwell Migration—COS7 cells were treated with control and ACK siRNAs for 48 h inclusive of 24-h serum starvation before detachment from culture dishes by trypsin. Excess trypsin was washed out. Cells were counted using a hemocytometer and diluted to a cell density of 2.5×10^5 cells/ml. The undersides of the transwells were precoated with 10 μg/ml of fibronectin in 37 °C incubator for at least 1 h and washed away with PBS. A volume of 100 μl of the cells were added to the top well and allowed for migration toward the underside of the well submerged in 600 μl of serum-free medium with 400 ng/ml GAS6 for 3 h in the 37 °C incubator. Thereafter, the migrated cells were fixed via 3% paraformaldehyde for 15 min. Non-migrated cells were scraped off via cotton swap. The membranes with the migrated cells were cut out of the well and stained with TRITC-phalloidin and Hoechst dye for 1 h before washing with 0.1% Triton-X/PBS four times. The membranes were placed onto glass slides with the cell facing up and mounted with mounting medium and coverslips. A Zeiss Axioplan2 microscope was used to view the cells and the number of nuclei per ×40 field was counted. At least 30 fields/membrane were quantitated.

Phase-contrast Imaging—Cells were transfected with control and ACK siRNAs for 24 h before detachment and reseeding at low density in 6-well plates and allowed for cell attachment (at least 5 h) before serum starvation overnight. Cells were imaged using Image Pro in a 37 °C, 5% CO_2 stage with ×32 lens through a Zeiss Axiovert-135M microscope. Images were taken around 5 min after GAS6 addition at a 40-s interval scan and with 2 fields/well and over a 90-min total time course.

Immunofluorescence Analysis—For RTK interaction analysis, cells were pretreated with 500 μM sodium orthovanadate for 30 min before fixation. Cells were fixed with 3% paraformaldehyde in PBS for at least 10 min and washed with PBS. Cells were permeabilized with 0.2% Triton X-100, PBS for 10 min and blocked with 1% fetal bovine serum in 0.1% Triton X-100, PBS for 10 min and blocked with 10% fetal bovine serum, PBS. Primary antibodies were diluted in 0.5% Triton X-100, PBS; incubated with the cells for at least 1 h at room temperature; and washed with 0.1% Triton X-100, PBS. Secondary antibodies (anti-mouse/rabbit Alexa-488 or Alexa-546; 1:500) were incubated and washed under similar conditions. Cells were mounted and viewed by a Zeiss Axioplan2 microscope coupled to a Coolsnap HQ camera (Roper Scientific) using a ×63 oil lens. Images were processed by Adobe Photoshop.

RESULTS

ACK1 Can Interact with a Number of Receptor Tyrosine Kinases—The proline-rich C termini of human ACK1 and the non-kinase adaptor protein MIG6 display regions of mutual homology (Fig. 1*A*). This region is also conserved in zebrafish ACK1. The EGFR binding domain of MIG6 (7), which lies C-terminal to the Grb2 binding sequences, contains two domains (*underlined* in *yellow* and *red*), which are sequence-related to ACK1. Since ACK1 has been identified as an interactor with EGFR, PDFR, and Mer, we hypothesized that this region may act as a generic receptor tyrosine kinase (RTK) binding domain. To test this, the proline-rich and EGFR binding domain of ACK1 (T1; Fig. 1*B*) was co-expressed with a number of full-length RTKs. The expression constructs chosen represented most RTK subfamilies. These co-transfection experiments with GST-ACK-T1 indicated very weak interaction with Axl, PDGFR, and LTK, which is poor even for a positive control PDGFR (Fig. 1*C*); the degree of receptor solubility (*i.e.* input) was a significant factor for some of these pull-downs. Both Axl and LTK exhibited detectable interaction with ACK1-T1 but at a level that suggested indirect binding.

The Axl subfamily consists of Mer, Axl, and Sky kinases. A Mer-ACK1 interaction was previously reported, although the basis for this interaction was not investigated (17). Comparing the primary sequence of the kinase domain illustrates the degree of similarity of some of these ACK1-associated RTKs and other related kinases. It seemed likely that ACK1-associated receptor might include Sky and ALK, based on their similarity to Axl and LTK, respectively (Fig. 1*D*). In this regard, LTK and ALK are part of the insulin receptor superfamily, but there are no reports of ACK1 interaction with this subfamily. The LTK is expressed predominantly in pre-B cells and neuronal tissues (21, 22), whereas ALK is highly expressed in developing nervous system (23).

Grb2 Is Required to Promote ACK1 Binding to Axl, LTK, and ALK Receptor Kinases—ACK1 has been identified as a binding partner of the adaptor protein Grb2 (6, 24, 25). Nonetheless, it is unclear whether the proline-rich regions might bind other SH3 proteins with better avidity. Grb2 can bind two motifs in

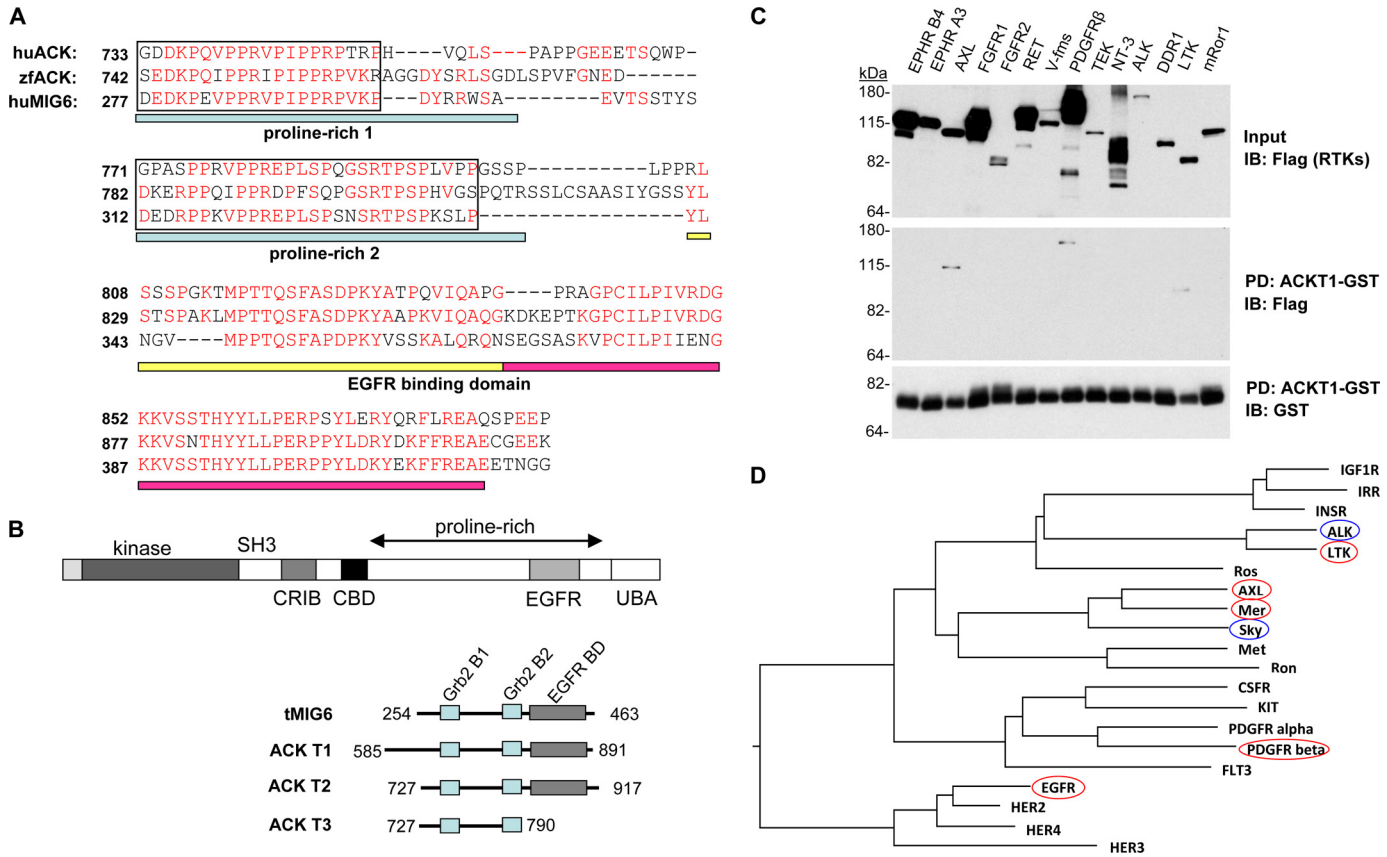

FIGURE 1. **Identification of RTKs that bind the region conserved between MIG6 and ACK1.** *A*, an alignment of the C-terminal regions of human ACK1 (*huACK1*), zebrafish ACK1 (*zfACK1*), and human MIG6 (*huMIG6*). The regions of conserved sequence are *highlighted* in *red*. *Blue bars below* represent the proline-rich regions that are implicated in Grb2 binding. *Yellow* and *pink bars* represent the segment 1 and segment 2 domains of MIG6 that were found to interact directly with EGFR (14). *B*, a schematic diagram of the multidomain structure of ACK1. *CRIB*, Cdc42 binding domain. A conserved clathrin binding domain (*CBD*) is followed by a region that is proline-rich. The ubiquitin association domain (*UBA*) is required for ubiquitination of ACK1 (20). An EGFR-binding region flanks this. The various truncated MIG6 and ACK1 constructs (tMIG6 and ACK1 T1, T2, and T3) used in this study are shown. *C*, screening of a panel of RTKs using the ACK T1 domain. GST-ACK T1 was co-expressed with FLAG-RTKs in COS7 cells, and the serum-starved cells were pretreated with vanadate (30 min) before lysis. Glutathione-Sepharose was used to pull down (*PD*) the ACK T1 and interacting RTKs. The exposure time for *top* and *middle panels* is identical. The *bottom panel* shows even recovery of GST-ACK1 T1. *D*, phylogenetic tree of the relationship between RTKs found to bind ACK1 and the relatedness of subfamilies. The *red circles* represent the positive ACK1 binders from the screen, and *blue circles* represent binders likely to bind ACK1 based on relatedness. *IB*, immunoblot.

the regions between the clathrin-binding and EGFR binding domain (Fig. 1*A*) (6). These well conserved proline-rich regions (with MIG6) were tested on *in vitro* SH3 arrays in order to assess which SH3 domains might represent optimal binders for these sequences (supplemental Fig. 1). The full data set will be discussed elsewhere,[3] but in this limited analysis of 34 SH3 domains, it is clear only Grb2 and Src family kinases are binders. Grb2 showed slightly better binding to the first proline-rich region of ACK1 (ACK1-(732–761)).

ACK1 interaction with EGFR and PDGR can be enhanced upon activation of the receptor (5, 7), consistent with an SH2-mediated process. On the basis that Grb2 might be limiting in our overexpression experiment, we tested the association of ACK-T1 in the presence and absence of HA-Grb2. Ror1 was included as a negative control because it was not detected in the first RTK screen (Fig. 1*B*). These experiments indicated that Grb2 greatly enhanced the ability of ACK-T1 to pull down the full-length LTK and ALK but not mouse Ror1 (*mRor1*; Fig. 2*A*).

Additional ACK1-associated RTK candidates were tested with ACK-T1 and a construct encompassing the C-terminal half of MIG6 termed tMIG6 (Fig. 1*B*). Co-expression of ACK-T1 with Grb2 enhanced the pull-down of Axl, LTK, and ALK significantly (Fig. 2*B*) but was less apparent with PDGFR and EGFR, thus indicating differences in the ways that ACK1 can be coupled to these receptors. It is notable that in a global study of proteins associated with EGFR, receptor activation was accompanied by only a 2-fold increase of bound ACK1 (26), suggesting that the binding is not primarily driven by SH2 interactions. It is known that PDGFR has no direct binding site for Grb2 and instead uses the adaptor tyrosine phosphatase Syp (27). Through this analysis, we point to differences in the avidity of interaction comparing ACK1 and MIG6. In particular, Grb2 did not impact on the interaction between tMIG6 and EGFR. It is noted that the Grb2 enhancement on ACK T1/EGFR interaction had a much lower -fold increment than that of Axl, ALK, and LTK and instead was similar to that of PDGFR. Although EGFR has a binding site for Grb2, we would suggest that the spatial arrangement is such that the proteins cannot form a productive trimeric complex. In the case of Axl, ALK, and LTK, it seems likely that the interaction of the Gb2 SH2 domain with phosphotyrosine and interaction of the Grb2 SH3 with ACK1 allows for binding of the EGFR binding domain

[3] W. Chan, unpublished results.

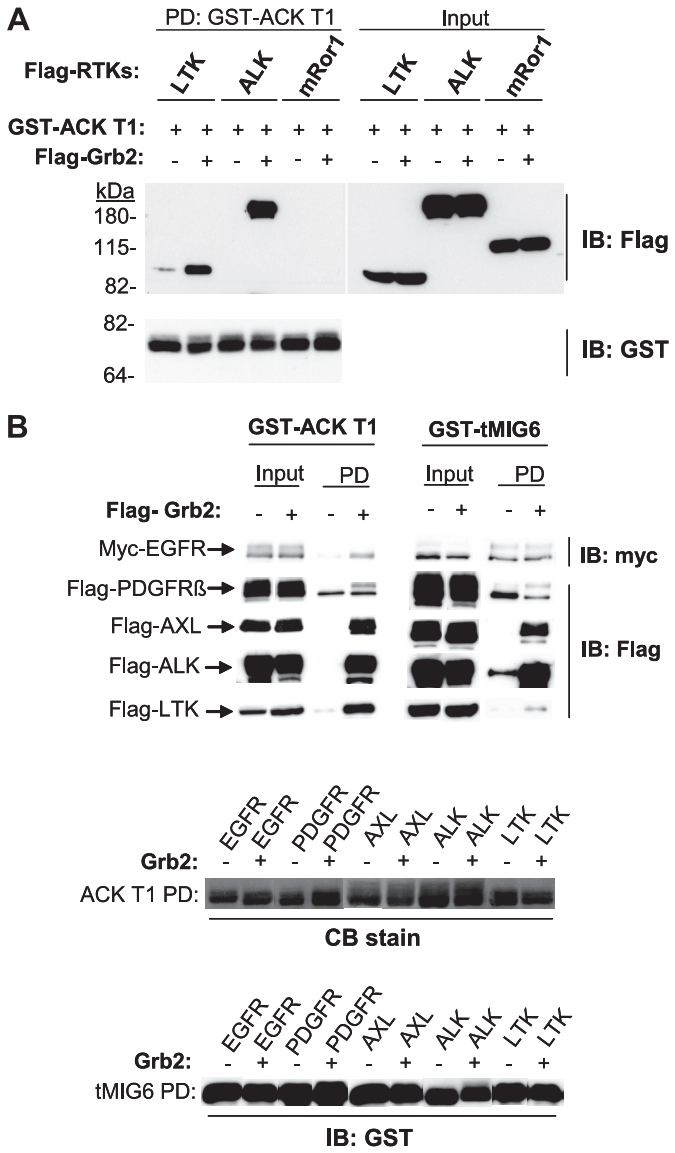

FIGURE 2. **Grb2 serves as a link between ACK1 and a number of RTKs.** *A*, LTK and ALK co-purify with ACK-T1 most efficiently in the presence of co-transfected Grb2. Constructs encoding human ALK, LTK, and mouse Ror1 (*mRor1*) were transfected as indicated into COS7 cells. These cells were also pretreated with vanadate (30 min) before lysis. The ability of GST-ACK T1 to pull down FLAG-tagged receptors was tested with and without co-expressed Grb2. The *lower panel* shows the level of GST-ACK T1 pull down. *B*, the requirement of Grb2 for ACK1 or MIG6 interaction varies. GST-ACK T1 or GST-tMIG6 were transfected with human cDNAs as shown; Myc-EGFR, FLAG-PDGFR, FLAG-Axl, FLAG-ALK, and FLAG-LTK were co-expressed with or without FLAG-Grb2. Proteins were recovered on glutathione-Sepharose and processed for Western blotting. The luminol exposure times are identical between input and GST pull-down panels. GST-ACK T1 and GST-tMIG6 levels were assessed by Coomassie Blue (*CB*) staining of the polyvinylidene difluoride membranes after transfer or blotted for anti-GST. *IB*, immunoblot.

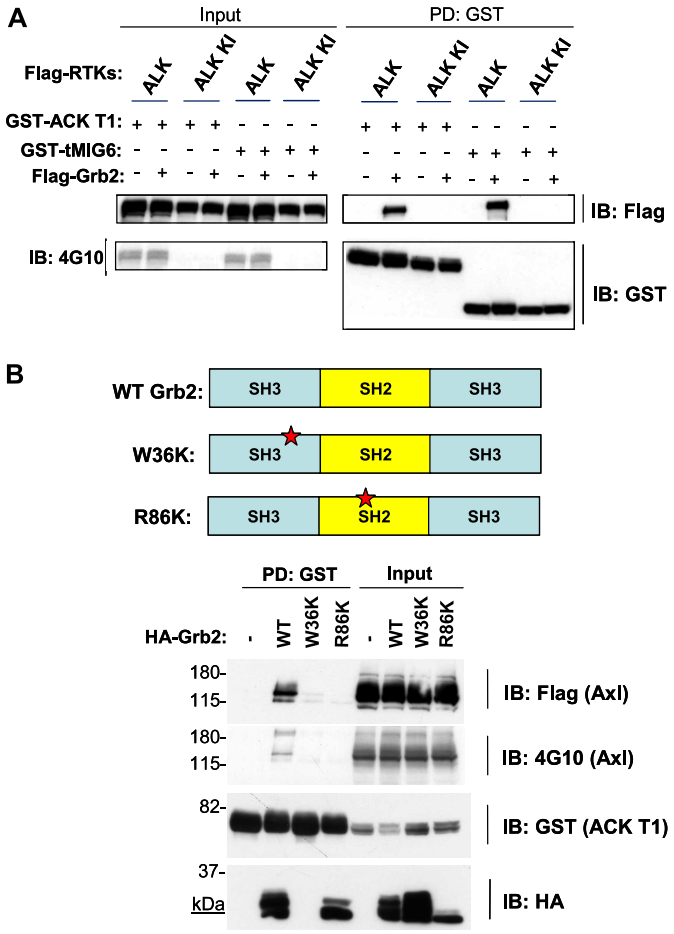

FIGURE 3. **ACK1 coupling to active receptors requires both Grb2 SH2 and SH3 domains.** *A*, FLAG-tagged ALK or kinase-inactive (*KI*) ALK was co-expressed with either GST-tMIG6 or GST-ACK T1 with or without Grb2. The *bottom two blots* represent the level of phosphotyrosine (4G10) and GST-ACK T1 or GTT-tMIG6. *B*, HA-tagged constructs of wild type Grb2 or loss of function mutants of the N-terminal SH3 Grb2(W36K) or SH2 domain Grb2(R86K) were co-expressed with FLAG-tagged Axl and GST-ACK T1. The ACK T1 pull-down was assessed for HA-Grb2 and FLAG-Axl by immunoblot as shown. Anti-phosphotyrosine (4G10) staining indicates that the receptor phosphorylation was similar in all cases. *IB*, immunoblot; *WT*, wild type.

with the equivalent regions of the kinase domain. With respect to LTK, it is apparent that ACK-T1-Grb2 was more efficient in binding LTK than the tMIG6-Grb2 complex. Again, these differences could arise from the affinity of the EGFR binding domain for LTK or the arrangement of this domain relative to the Grb2 binding sites.

Receptor Binding to ACK1 Is Dependent on Their Activation and Grb2 SH2 Interaction—To investigate further the mode of Grb2 binding, two approaches were employed to test the role of the SH3 and SH2 domains of Grb2. In the first, wild type and kinase-inactive ALK were compared for their ability to bind ACK-T1 or tMIG6 in the presence of Grb2. The inactive ALK (Fig. 3*A*, *lanes 3* and *4* and *lanes 7* and *8*) could not form a trimeric complex in either case. Thus, direct kinase-tMIG6 interactions are not detected in this assay, unlike with EGFR (14). In a second approach (Fig. 3*B*), we created two point mutants of Grb2 in the N-terminal SH3 (W36K) or SH2 domain (R86K) and tested their ability to mediate interaction between ACK-T1 and Axl. Neither Grb2 mutant was able to promote binding of ACK-T1 with Axl. The Grb2 R86K SH2 mutant bound ACK-T1 as expected (*bottom*) but did not allow the Axl complex. These effects are unrelated to any perturbation of the receptor activation because levels of receptor phosphotyrosine were equivalent.

To test the contribution of the Grb2 binding site *versus* the EGFR binding domain, we employed additional GST-ACK1 fragments (*cf.* Fig. 1*B*). Comparing ACK-T2 *versus* ACK-T3 (see Fig. 1*A*) and the level of Axl recovered in the GST pull-

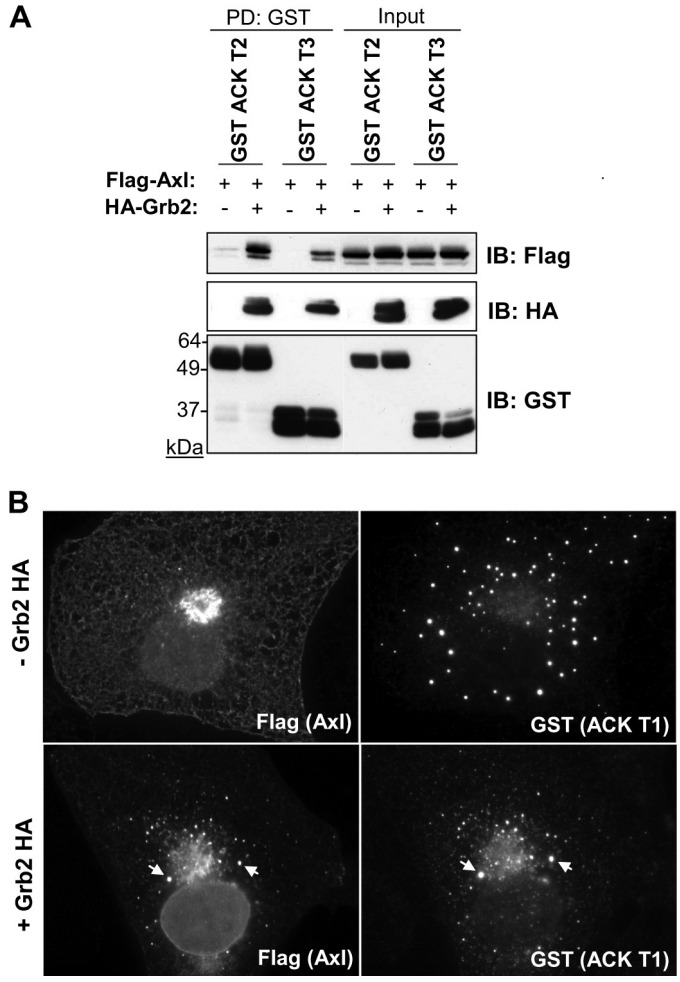

FIGURE 4. **EGFR binding domain and Grb2 binding domains of ACK1 cooperate to bind Axl.** *A*, two constructs encoding GST fused to ACK1 designated ACK1T2 and ACK1 T3 were employed (see Fig. 1*B*). These construct were co-expressed with FLAG-Axl with and without HA-Grb2. The GST-ACK fragments were assessed by Western blotting for levels of associated proteins. *B*, immunofluorescence staining of COS7 cells expressing ACK T1 and Axl show that the proteins significantly colocalized only with additional Grb2. Cells were pretreated with vanadate (30 min) before fixation. The *top panels* represent expression of GST-ACK T1 and FLAG-Axl, and the *bottom panels* include Grb2. The *white arrows* point out colocalized vesicles. *IB*, immunoblot.

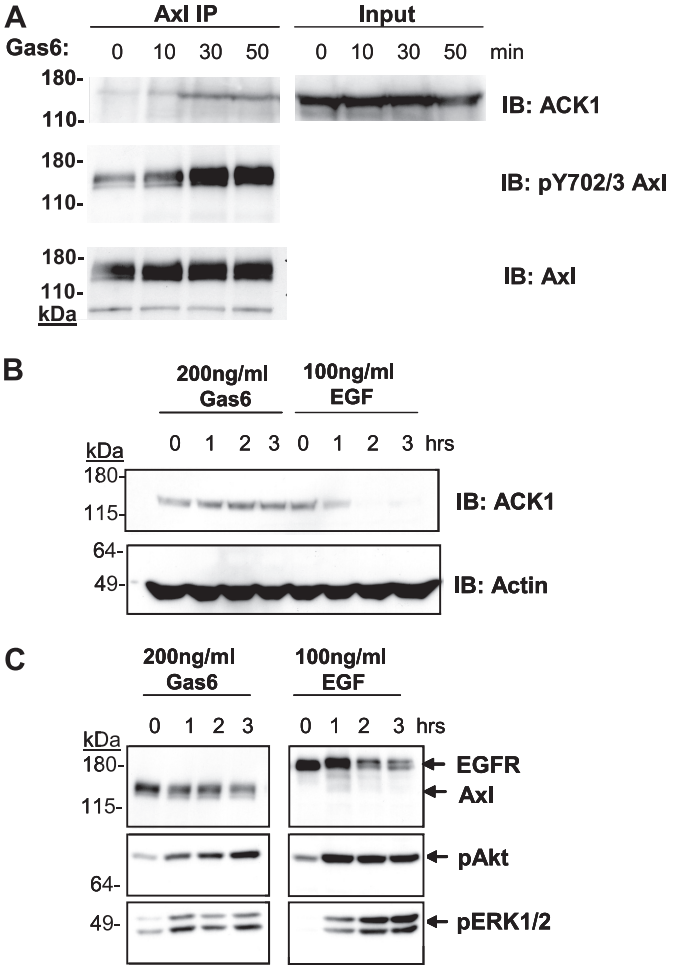

FIGURE 5. **Endogenous ACK1 interacts with Axl and have different effects from EGFR signaling on ACK1 turnover.** *A*, ACK1 interacts with endogenous Axl in an activation-dependent manner. Serum-starved COS7 cells were treated with GAS6 (400 ng/ml) and lysed at the various time points indicated. Endogenous Axl was immunoprecipitated (*IP*) and immunoblotted (*IB*) for interacting ACK1. GAS6 treatment induces Axl autophosphorylation of Tyr^{702}/Tyr^{703} residues in the activation loop. Immunoblotting of phospho-Tyr^{702}/Tyr^{703} demonstrates an increase in Axl activation over time of GAS6 treatment and plateaus by 30 min. *B*, Axl and EGFR signaling have different effects on ACK1 turnover. EGF but not GAS6 treatment induces ACK1 turnover. COS7 cells were serum-starved overnight and treated with 100 ng/ml EGF or 200 ng/ml GAS6 and then lysed at the time points indicated. The cell lysates were separated by SDS-PAGE and probed with anti-ACK1 or anti-actin (loading control). *C*, Western analysis of EGFR and Axl and the activation of downstream targets indicated by levels of phospho-Akt (*pAkt*) (Ser^{473}) and phospho-ERK1/2 (*pERK1/2*) (activation loop).

downs, we conclude that the so-called EGFR binding domain (Fig. 1) does contribute to binding. These experiments indicate that Axl and probably other RTKs that we have identified as "ACK1 binders" are complexed to ACK1 at low affinity when the receptor is in an inactive state but can recruit ACK1 upon receptor activation and Grb2 binding. To further confirm that the trimeric ACK1-Grb2-Axl complex could be seen in cells, immunofluorescence staining of the overexpressed proteins was performed (Fig. 4*B*). The Axl receptor is predominantly perinuclear with lower levels found across the plasma membrane. In the absence of Grb2, ACK-T1 staining is localized in puncta without Axl staining. Co-expression of Grb2 resulted in colocalization of Axl and ACK1 in vesicle-like structures (*arrows*).

The overexpression results clearly point to a requirement for Grb2 in mediating ACK1-RTK interactions. The ability of ACK1 to bind Axl in particular was corroborated by the detection of endogenous interaction between activated Axl and ACK1 in COS7 cells (Fig. 5*A*). These cells express ACK1 and Axl at levels equivalent to or higher than other lines we tested (see Fig. 8*A*). Endogenous Axl was activated by the ligand GAS6 (growth arrest-specific gene 6), and the receptor was immunoprecipitated. Since ACK1 interacts with Axl in a Grb2-dependent manner, it is important to assess that the interaction was activation-dependent. The activation loop phosphorylation sites in Mer (Tyr^{753} and Tyr^{754}) have been shown to be critical for kinase activity (28). Because no antibody has been reported to monitor Axl activation status, a 13-residue phosphopeptide containing phospho-Tyr^{702}/Tyr^{703} (analogous to this Mer site) was used to generate an antibody to the activation loop of Axl. GAS6 treatment results in increasing modification of Axl Tyr^{702}/Tyr^{703}; under these conditions, the amount of co-im-

munoprecipitated ACK1 correlated with Axl activation and peaked at 50 min (Fig. 5*A*).

EGFR and Axl Have Different Effects on ACK1 Turnover—EGFR activation leads to activation-dependent turnover of ACK1 (20), with more rapid loss of ACK1 than EGFR itself. This process is driven by interaction of ACK1 with the E3 ligase Nedd4. To test if activation of Axl also drives ACK1 degradation, we compared EGF and GAS6 treatments of COS7 cells. Serum-starved cells were treated with EGF or GAS6; as expected, ACK1 levels decreased significantly by 2 h after EGF treatment (Fig. 5*B*), but GAS6 treatment failed to affect ACK1 levels even after 3 h. In both cases, generation of active forms of Akt and ERK suggested that these downstream pathways are not involved in ACK1 turnover (Fig. 5*C*). Thus, we conclude that the differential mode of interactions between ACK1 and the two receptors (Fig. 2*B*) leads to different outcomes in terms of down-regulation of ACK1. It is interesting to note that in 32D cells expressing Axl, GAS6-stimulated Axl activation failed to elicit a mitogenic response or ERK activation, although an EFFR (extracellular domain)-Axl chimera was potent in both assays (29).

ACK1 Affects Axl Degradation in Response to GAS6—ACK1 is implicated in the ligand-dependent degradation of EGFR (5), and it was therefore of interest to investigate how the ACK1 kinase affects Axl turnover. Overexpression of full-length ACK1 globally disrupts clathrin and thus interferes with the transport and function of many receptors (4, 11). To study the physiological role of the interaction of these kinases, we down-regulated ACK1 by siRNA (*cf.* Fig. 7*A*). Upon GAS6-induced Axl activation, the total receptor levels dropped to ~35% of starting levels by 90 min. In ACK1 siRNA-treated cells, ~95% of Axl remained at 90 min (average of three experiments; Fig. 6*A*). Given the requirement for Grb2 in ACK1 coupling to Axl (Fig. 3*B*), knockdown of Grb2 was also examined; control or Grb2-targeted siRNA treatments (48 h) were compared for their effects on ligand-induced Axl turnover (Fig. 6*B*). With reduced Grb2 levels, we again observed a block of the GAS6-mediated Axl turnover. This was surprising because the siRNA used (30) was relatively ineffective in our hands (~50% reduction) but points to a central role of Grb2 and ACK1 in this process. Because Grb2 is used by multiple signaling pathways, it is possible that its level is limiting in this signaling context. These observations suggest the interplay between Axl, Grb2, and ACK1 plays a key role in ligand-mediated Axl degradation.

ACK1 Promotes GAS6-mediated ERK Activation—Grb2 is well known for its association with SOS, a key activator of Ras, leading to activation of the Raf/MEK/ERK pathway (31–33). Association of ACK1 with the SH3 domains of Grb2 suggested competition with Grb2-mediated ERK activation. ACK1 knockdown cells were evaluated for the ability of GAS6 to induce ERK activation. Interestingly, silencing of ACK1 results in a reproducible reduction of ERK1/2 activation (Fig. 7, *A* and *B*), which was statistically significant ($T = 15$ min, $p = 0.061$; $T = 45$ min, $p = 0.018$; Student's t test). This suggests in turn that ACK1 binding to Axl promotes GAS6-mediated ERK activation. We confirmed that GAS6-induced Axl activation itself was normal after ACK1 silencing (Fig. 7*C*). This presents an intriguing situation where ACK1 is required to mediate down-regulation of Axl upon acute GAS6 signaling yet actually serves to promote downstream ERK signaling.

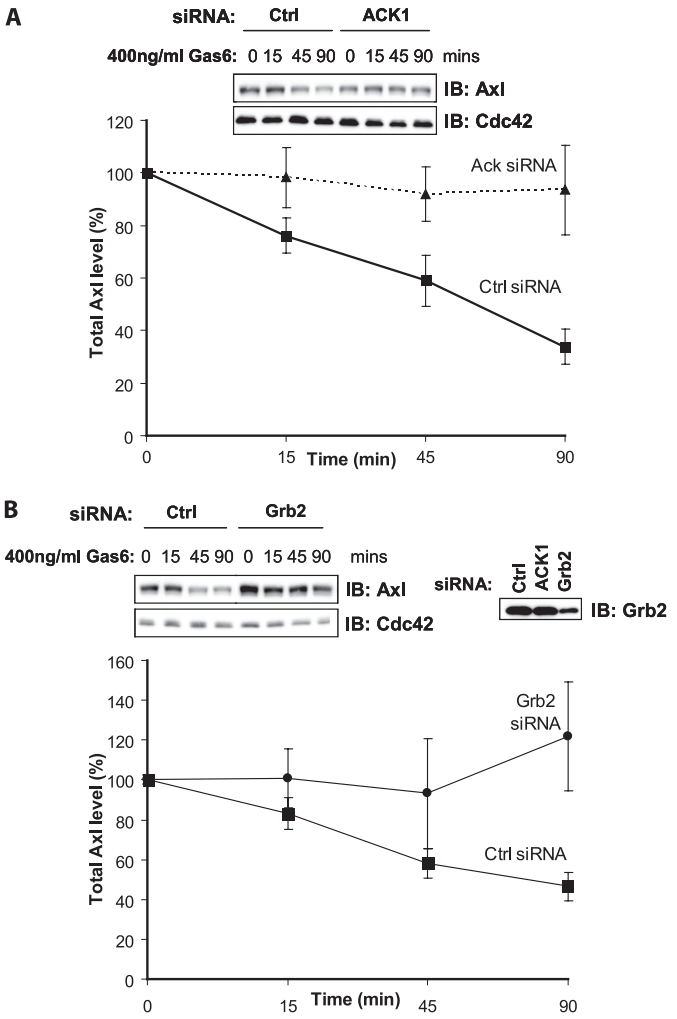

FIGURE 6. **ACK1 regulates GAS6-induced turnover of Axl.** *A*, ACK1 is required for GAS6-induced Axl degradation. COS7 cells were transfected with either control (*Ctrl*) siRNA or ACK1 siRNAs for 24 h and serum-starved for a further 24 h. After the addition of 400 ng/ml GAS6, lysates were harvested and analyzed with anti-Axl and anti-Cdc42 (loading control). Quantitation of the bands was carried out with ImageJ. *B*, Grb2 contribute to GAS6-induced Axl degradation. COS7 cells were treated with control siRNA or Grb2 siRNA and serum-starved before GAS6 treatment and lysis. The lysates were analyzed via anti-Axl and anti-Cdc42 (loading control). Immunoblot of Grb2 exhibits the efficacy of the Grb2 siRNA. Image J was employed to quantitate the bands. Similarly, the Western blot bands were quantitated using ImageJ. *IB*, immunoblot.

Loss of ACK1 Suppresses Normal Membrane Dynamics and Cell Migration—The human DU145 prostate cancer cell line was chosen for additional experiments (Fig. 8) because the morphology of these cells is more uniform than for COS7 lines. ACK1 has been implicated in promoting cell migration and metastasis of tumors (10, 18). We first investigated the effect of ACK1 silencing on GAS6-induced ruffling by standard time lapse phase-contrast microscopy. Serum-starved DU145 cells generate membrane ruffles within minutes upon GAS6 treatment. By contrast, the ACK1 knockdown cells rarely exhibited phase-dark peripheral ruffles, as illustrated in Fig. 8*B*. In COS7 cells, GAS6 treatment gave robust and dynamic ruffles, which were much less obvious in ACK1 knockdown cells (data not

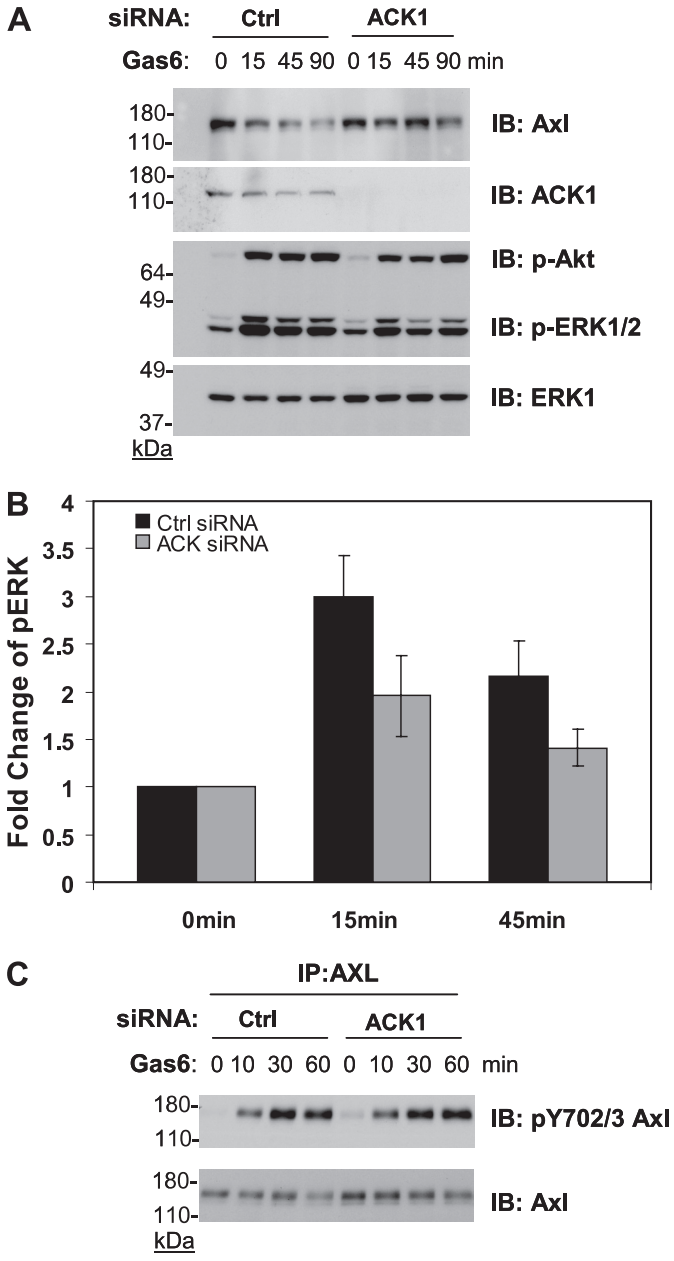

FIGURE 7. **ACK1 promotes GAS6-mediated ERK activation.** *A*, COS7 cells were transfected with either control (*Ctrl*) siRNA or ACK1 siRNAs (siA_2 and siC) for 24 h and serum-starved 24 h before GAS6 treatment. The lysates were probed with antibodies against phospho-p44/p42 and phospho-Akt for Axl signaling analysis. Total ERK1 was immunoblotted (*IB*) as loading control. Immunoblots of Axl and ACK1 demonstrate the activity of GAS6 and efficacy of ACK siRNAs, respectively. *B*, ACK1 knock-down cells demonstrate significant reduction in ERK activation at $T = 15$ and 45 min. Quantitation of the normalized phospho-ERK for $T = 0–45$ min was performed via ImageJ, and -fold increment was based on time 0 value for control and ACK1 siRNA-treated samples. *C*, silencing of ACK1 has negligible effect on Axl activation. Serum-starved COS7 cells that were treated with either control siRNA or ACK1 siRNAs were induced by GAS6 before immunoprecipitation (*IP*) of Axl. Immunoblotting of Axl from control and ACK1 knockdown cells demonstrates no difference in Tyr^{702}/Tyr^{703} phosphorylation.

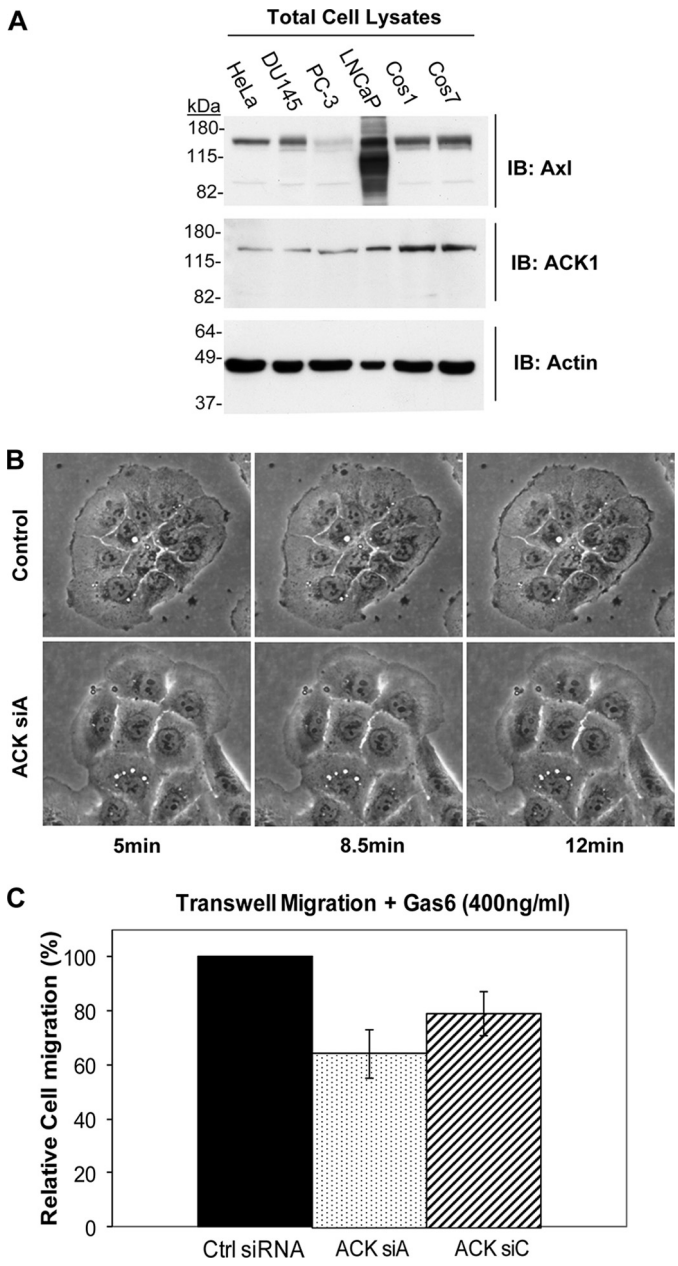

FIGURE 8. **ACK1 promotes cell ruffling and migration.** *A*, expression of ACK1 and Axl in cultured cell lines. Cells as shown were immunoblotted with anti-Axl and ACK1. Immunoblotting (*IB*) of actin was used as the loading control. *B*, ACK1 is required for GAS6-induced cell ruffling. Phase-contrast images of DU145 cells at 40-s intervals after GAS6 addition. Images of cells representing control and ACK1 knock-down cells are shown. *C*, silencing of ACK1 reduces cell migration. COS7 cells were incubated with siRNAs for 24 h and then serum-starved for 24 h. These cells (2.5×10^4) were added to the top well of a modified Boyden chamber (8-μm pore) and were assessed for migration (at 3 h) to the lower side coated with fibronectin, under the influence of 400 ng/ml GAS6. Cells were stained with phalloidin, and cell nuclei/field were counted (×40 objective). *Ctrl*, control.

shown). In monolayer scratch assays, we noted that the leading edge of ACK1 knockdown cells was more uniform, with Rac1 itself evenly distributed along this edge (supplemental Fig. 2). Control COS7 cells exhibited more dynamic cell protrusions. We note that Cdc42-driven migration and $p130^{cas}$ phosphorylation have been linked to ACK1 signaling (9, 10). The effect of ACK1 knockdown in Boyden chamber migration showed that ACK1 knockdown reduced cell migration (Fig. 8*C*), as has been reported for EGF-mediated cell migration (9, 34). Thus, ACK1 may have a general role of coupling RTKs to cell movement.

DISCUSSION

ACK1 is implicated in trafficking via its association with clathrin, Grb2 and SNX9 (4, 6, 25). EGFR transport and endo-

cytosis is one of the best understood among RTK systems and involves many clathrin-associated adaptors (as reviewed in Ref. 35). The potential role for ACK1 to modulate RTK trafficking is interesting, given its amplification and association with prostate cancer metastasis (7). Our study broadens the potential RTK partners for ACK1 and points perhaps to a more general role for ACK1 on RTK signaling. We show here that there is Grb2-dependent coupling of ACK1 with Axl family kinases and the insulin receptor-like kinases LTK and ALK. We have yet to test insulin receptor itself.

This is the first report to directly compare the efficacy of ACK1 and MIG6 binding to EGFR with and without Grb2. We suggest that EGFR binds better to MIG6 than ACK1 (when we use smaller soluble constructs), and in neither case is the binding significantly stimulated by Grb2 (Fig. 2*B*). With full-length ACK1, >90% of the kinase is Triton X-100-insoluble, which precludes meaningful analysis (data not shown). Structural studies of the MIG6 complexed to the EGFR kinase domain indicates a large protein interface (14). ACK1 binds more weakly to EGFR and the adaptor role of Grb2 in our experiments (Fig. 2) fits with observations that PDGFR has no direct Grb2 binding site (27). By contrast Axl, LTK, and ALK binding to ACK1 and MIG6 is strongly augmented by Grb2 expression, where the adaptor is obviously limiting in these overexpression experiments. It is interesting to note that in the presence of additional Grb2, LTK binds much better to ACK1 than MIG6. Given the homology across the region of ACK1 and MIG6 (Fig. 1*A*), it seems likely that they bind Axl and ALK through the same set of interactions. We have shown that Grb2 cooperates with the receptor binding domain of ACK1 to bind Axl (Fig. 4*A*) and probably binds LTK and ALK in the same manner. ACK1 levels are down-regulated by EGF treatment and not GAS6. The turnover is driven by association of activated ACK1 with Nedd4-2, and proteosomal degradation (20). Thus, one possibility to explain our result is that GAS6-Axl is coupled to ACK1 but is not a good activator of ACK1 kinase; unfortunately, there are presently no available tools to test this. The GAS6/Axl axis has important roles in leukemia, cell survival, proliferation, and migration, and thus its interplay with ACK1 is of considerable interest (36–39).

Axl was originally identified as a transforming gene in hematological malignancies (36, 40, 41). The expression of GAS6, the ligand of Axl, can be up-regulated in growth-arrested cells (42, 43). GAS6/Axl signaling is linked to cell survival and proliferation; Axl, like many RTKs, acts on pathways that involve PI3K, ERK, and NF-κB (37, 44–47). GAS6 induces proliferation of cardiac fibroblast, prostate cancer cells, and mammary cells primarily via ERK (39, 48, 49). With respect to migration, GAS6/Axl signaling increases gonadotropin-releasing hormone neuronal cell migration through Rac1, p38 MAPK, and MAPK-activated protein kinase 2 (38), but it is unclear how Axl distinguishes itself from other RTKs with respect to Rac1 activation.

Axl is overexpressed in a variety of cancer cell lines of breast, colon, thyroid, melanoma, and prostate origins (50–54). The increased activity of Axl in tumors would promote typical hallmarks of cancer cells, namely inappropriate cell cycle reentry, cell survival, and cell transformation (55–57). Increased levels of Axl in the DU145 cell line is suggested to correlate with its metastatic behavior as for several primary tumors (58, 59). More recently, Axl overexpression detected in pancreatic adenocarcinomas correlated with increased prevalence of lymph node metastases (34). ACK1 has been implicated in promoting cancer metastasis (17, 18). The ability of ACK1 to promote MAPK signaling and cell migration (Figs. 7 and 8) suggests that ACK1 positively promotes the function of Axl and other RTKs in tumor cells. The ALK receptor kinase is causative in anaplastic large cell lymphomas in which there is fusion at its N terminus with NPM (60, 61).

Similar to the role of ACK1 on EGFR turnover (5, 15), silencing of ACK1 also resulted in the loss of GAS6-induced Axl depletion. Investigations into the localization of Axl indicate that in normal and ACK1 knockdown cells, the disposition of Axl receptor is not significantly different (data not shown). Grb2 is implicated in the clathrin-mediated endocytosis of activated EGFR (30); in this study, we show that Grb2 is also required for Axl turnover. The involvement of Cdc42, which binds to the CRIB domain of ACK1, in Axl turnover (data not shown) suggests that the GTPases (perhaps through ACK1) plays a role in Axl down-regulation. Although ACK1 promotes Axl down-regulation, it also appears to enhance MAPK activation (Fig. 8). One explanation might involve a requirement for clathrin-mediated endocytosis for efficient Axl signaling (62, 63). It is now clear that Ras/MAPK signaling can occur in various endomembrane compartments (64, 65). Hence, by promoting Axl trafficking, ACK1 might serve to promote signaling through the MAPK pathway.

Our working hypothesis is that ACK1 regulates the ubiquitination of associated receptors. The effects of ACK1 silencing also suggest a role for ACK1 in regulating Rac1. This is consistent with the reduced migration of ACK1 siRNA-treated cells in the transwell assay. These effects on cell migration might be the result of altered $p130^{cas}$ signaling, but further studies of this key adaptor (10) are required; because $p130^{cas}$ links to Crk and DOCK180 (66, 67), an effect on Rac1 is expected.

In conclusion, our findings suggest that a range of receptor tyrosine kinases are modulated by the non-receptor kinase ACK1 and that the effect of abnormally high levels of ACK1 is likely to modify the output from these RTKs upon ligand-induced stimulation with resultant aberrant downstream signaling.

Acknowledgments—We thank the following individuals for cDNA clones encoding the following receptor tyrosine kinases: Dr. B. Souttou, Dr. B. Leitinger, Dr. K. Nakamura, and Dr. A. Nomachi for providing the constructs of ALK, DDR1, LTK, and mouse Ror1, respectively.

REFERENCES

1. Manser, E., Leung, T., Salihuddin, H., Tan, L., and Lim, L. (1993) *Nature* **363,** 364–367
2. Hoehn, G. T., Stokland, T., Amin, S., Ramírez, M., Hawkins, A. L., Griffin, C. A., Small, D., and Civin, C. I. (1996) *Oncogene* **12,** 903–913
3. Hackel, P. O., Gishizky, M., and Ullrich, A. (2001) *Biol. Chem.* **382,** 1649–1662
4. Teo, M., Tan, L., Lim, L., and Manser, E. (2001) *J. Biol. Chem.* **276,** 18392–18398
5. Shen, F., Lin, Q., Gu, Y., Childress, C., and Yang, W. (2007) *Mol. Biol. Cell*

18, 732–742
6. Yeow-Fong, L., Lim, L., and Manser, E. (2005) *FEBS Lett.* **579,** 5040–5048
7. Galisteo, M. L., Yang, Y., Ureña, J., and Schlessinger, J. (2006) *Proc. Natl. Acad. Sci. U.S.A.* **103,** 9796–9801
8. Lougheed, J. C., Chen, R. H., Mak, P., and Stout, T. J. (2004) *J. Biol. Chem.* **279,** 44039–44045
9. Eisenmann, K. M., McCarthy, J. B., Simpson, M. A., Keely, P. J., Guan, J. L., Tachibana, K., Lim, L., Manser, E., Furcht, L. T., and Iida, J. (1999) *Nat. Cell Biol.* **1,** 507–513
10. Modzelewska, K., Newman, L. P., Desai, R., and Keely, P. J. (2006) *J. Biol. Chem.* **281,** 37527–37535
11. Yang, W., Lin, Q., Guan, J. L., and Cerione, R. A. (1999) *J. Biol. Chem.* **274,** 8524–8530
12. Fiorentino, L., Pertica, C., Fiorini, M., Talora, C., Crescenzi, M., Castellani, L., Alemà, S., Benedetti, P., and Segatto, O. (2000) *Mol. Cell. Biol.* **20,** 7735–7750
13. Anastasi, S., Fiorentino, L., Fiorini, M., Fraioli, R., Sala, G., Castellani, L., Alemà, S., Alimandi, M., and Segatto, O. (2003) *Oncogene* **22,** 4221–4234
14. Zhang, X., Pickin, K. A., Bose, R., Jura, N., Cole, P. A., and Kuriyan, J. (2007) *Nature* **450,** 741–744
15. Grøvdal, L. M., Johannessen, L. E., Rødland, M. S., Madshus, I. H., and Stang, E. (2008) *Exp. Cell Res.* **314,** 1292–1300
16. Hopper, N. A., Lee, J., and Sternberg, P. W. (2000) *Mol. Cell* **6,** 65–75
17. Mahajan, N. P., Whang, Y. E., Mohler, J. L., and Earp, H. S. (2005) *Cancer Res.* **65,** 10514–10523
18. van der Horst, E. H., Degenhardt, Y. Y., Strelow, A., Slavin, A., Chinn, L., Orf, J., Rong, M., Li, S., See, L. H., Nguyen, K. Q., Hoey, T., Wesche, H., and Powers, S. (2005) *Proc. Natl. Acad. Sci. U.S.A.* **102,** 15901–15906
19. Hafizi, S., and Dahlbäck, B. (2006) *Cytokine Growth Factor Rev.* **17,** 295–304
20. Chan, W., Tian, R., Lee, Y. F., Sit, S. T., Lim, L., and Manser, E. (2009) *J. Biol. Chem.* **284,** 8185–8194
21. Ben-Neriah, Y., and Bauskin, A. R. (1988) *Nature* **333,** 672–676
22. Maru, Y., Hirai, H., and Takaku, F. (1990) *Oncogene Res.* **5,** 199–204
23. Iwahara, T., Fujimoto, J., Wen, D., Cupples, R., Bucay, N., Arakawa, T., Mori, S., Ratzkin, B., and Yamamoto, T. (1997) *Oncogene* **14,** 439–449
24. Lev, S., Moreno, H., Martinez, R., Canoll, P., Peles, E., Musacchio, J. M., Plowman, G. D., Rudy, B., and Schlessinger, J. (1995) *Nature* **376,** 737–745
25. Satoh, T., Kato, J., Nishida, K., and Kaziro, Y. (1996) *FEBS Lett.* **386,** 230–234
26. Blagoev, B., Ong, S. E., Kratchmarova, I., and Mann, M. (2004) *Nat. Biotechnol.* **22,** 1139–1145
27. Li, W., Nishimura, R., Kashishian, A., Batzer, A. G., Kim, W. J., Cooper, J. A., and Schlessinger, J. (1994) *Mol. Cell. Biol.* **14,** 509–517
28. Ling, L., Templeton, D., and Kung, H. J. (1996) *J. Biol. Chem.* **271,** 18355–18362
29. Fridell, Y. W., Jin, Y., Quilliam, L. A., Burchert, A., McCloskey, P., Spizz, G., Varnum, B., Der, C., and Liu, E. T. (1996) *Mol. Cell. Biol.* **16,** 135–145
30. Jiang, X., Huang, F., Marusyk, A., and Sorkin, A. (2003) *Mol. Biol. Cell* **14,** 858–870
31. Buday, L., and Downward, J. (1993) *Cell* **73,** 611–620
32. Chardin, P., Camonis, J. H., Gale, N. W., van Aelst, L., Schlessinger, J., Wigler, M. H., and Bar-Sagi, D. (1993) *Science* **260,** 1338–1343
33. Gale, N. W., Kaplan, S., Lowenstein, E. J., Schlessinger, J., and Bar-Sagi, D. (1993) *Nature* **363,** 88–92
34. Howlin, J., Rosenkvist, J., and Andersson, T. (2008) *Breast Cancer Res.* **10,** R36
35. Sorkin, A., and Goh, L. K. (2008) *Exp. Cell Res.* **314,** 3093–3106
36. Liu, E., Hjelle, B., and Bishop, J. M. (1988) *Proc. Natl. Acad. Sci. U.S.A.* **85,** 1952–1956
37. Goruppi, S., Ruaro, E., Varnum, B., and Schneider, C. (1997) *Mol. Cell Biol.* **17,** 4442–4453
38. Allen, M. P., Linseman, D. A., Udo, H., Xu, M., Schaack, J. B., Varnum, B., Kandel, E. R., Heidenreich, K. A., and Wierman, M. E. (2002) *Mol. Cell Biol.* **22,** 599–613
39. Sainaghi, P. P., Castello, L., Bergamasco, L., Galletti, M., Bellosta, P., and Avanzi, G. C. (2005) *J. Cell Physiol.* **204,** 36–44
40. Schmitz, A. A., Govek, E. E., Böttner, B., and Van Aelst, L. (2000) *Exp. Cell Res.* **261,** 1–12
41. Lin, M., and van Golen, K. L. (2004) *Breast Cancer Res. Treat.* **84,** 49–60
42. Schneider, C., King, R. M., and Philipson, L. (1988) *Cell* **54,** 787–793
43. Manfioletti, G., Brancolini, C., Avanzi, G., and Schneider, C. (1993) *Mol. Cell Biol.* **13,** 4976–4985
44. Hasanbasic, I., Cuerquis, J., Varnum, B., and Blostein, M. D. (2004) *Am. J. Physiol. Heart Circ. Physiol.* **287,** H1207–H1213
45. Goruppi, S., Ruaro, E., Varnum, B., and Schneider, C. (1999) *Oncogene* **18,** 4224–4236
46. Lee, W. P., Wen, Y., Varnum, B., and Hung, M. C. (2002) *Oncogene* **21,** 329–336
47. Demarchi, F., Verardo, R., Varnum, B., Brancolini, C., and Schneider, C. (2001) *J. Biol. Chem.* **276,** 31738–31744
48. Stenhoff, J., Dahlbäck, B., and Hafizi, S. (2004) *Biochem. Biophys. Res. Commun.* **319,** 871–878
49. Goruppi, S., Chiaruttini, C., Ruaro, M. E., Varnum, B., and Schneider, C. (2001) *Mol. Cell Biol.* **21,** 902–915
50. Shieh, Y. S., Lai, C. Y., Kao, Y. R., Shiah, S. G., Chu, Y. W., Lee, H. S., and Wu, C. W. (2005) *Neoplasia* **7,** 1058–1064
51. Quong, R. Y., Bickford, S. T., Ing, Y. L., Terman, B., Herlyn, M., and Lassam, N. J. (1994) *Melanoma Res.* **4,** 313–319
52. Chen, W. S., Kung, H. J., Yang, W. K., and Lin, W. (1999) *Int. J. Cancer* **83,** 579–584
53. Ito, T., Ito, M., Naito, S., Ohtsuru, A., Nagayama, Y., Kanematsu, T., Yamashita, S., and Sekine, I. (1999) *Thyroid* **9,** 563–567
54. Meric, F., Lee, W. P., Sahin, A., Zhang, H., Kung, H. J., and Hung, M. C. (2002) *Clin. Cancer Res.* **8,** 361–367
55. Lin, W. C., Li, A. F., Chi, C. W., Chung, W. W., Huang, C. L., Lui, W. Y., Kung, H. J., and Wu, C. W. (1999) *Clin. Cancer Res.* **5,** 1745–1751
56. Challier, C., Uphoff, C. C., Janssen, J. W., and Drexler, H. G. (1996) *Leukemia* **10,** 781–787
57. Berclaz, G., Altermatt, H. J., Rohrbach, V., Kieffer, I., Dreher, E., and Andres, A. C. (2001) *Ann. Oncol.* **12,** 819–824
58. Jacob, A. N., Kalapurakal, J., Davidson, W. R., Kandpal, G., Dunson, N., Prashar, Y., and Kandpal, R. P. (1999) *Cancer Detect. Prev.* **23,** 325–332
59. Craven, R. J., Xu, L. H., Weiner, T. M., Fridell, Y. W., Dent, G. A., Srivastava, S., Varnum, B., Liu, E. T., and Cance, W. G. (1995) *Int. J. Cancer* **60,** 791–797
60. Morris, S. W., Kirstein, M. N., Valentine, M. B., Dittmer, K. G., Shapiro, D. N., Saltman, D. L., and Look, A. T. (1994) *Science* **263,** 1281–1284
61. Shiota, M., Nakamura, S., Ichinohasama, R., Abe, M., Akagi, T., Takeshita, M., Mori, N., Fujimoto, J., Miyauchi, J., Mikata, A., Nanba, K., Takami, T., Yamabe, H., Takano, Y., Izumo, T., Nagatani, T., Mohri, N., Nasu, K., Satoh, H., Katano, H., Fujimoto, J., Yamamoto, T., and Mori, S. (1995) *Blood* **86,** 1954–1960
62. Kranenburg, O., Verlaan, I., and Moolenaar, W. H. (1999) *J. Biol. Chem.* **274,** 35301–35304
63. Vieira, A. V., Lamaze, C., and Schmid, S. L. (1996) *Science* **274,** 2086–2089
64. Chiu, V. K., Bivona, T., Hach, A., Sajous, J. B., Silletti, J., Wiener, H., Johnson, R. L., 2nd, Cox, A. D., and Philips, M. R. (2002) *Nat. Cell Biol.* **4,** 343–350
65. Fehrenbacher, N., Bar-Sagi, D., and Philips, M. (2009) *Mol. Oncol.* **3,** 297–307
66. Webb, D. J., Donais, K., Whitmore, L. A., Thomas, S. M., Turner, C. E., Parsons, J. T., and Horwitz, A. F. (2004) *Nat. Cell Biol.* **6,** 154–161
67. Gustavsson, A., Yuan, M., and Fällman, M. (2004) *J. Biol. Chem.* **279,** 22893–22901